CHAPTER 4

INSTABILITY AND THE PRODUCTION OF TURBULENCE

In this chapter we consider various mechanisms whereby laminar flows of a stably stratified fluid can break down and become turbulent. The first task is to summarize some results of hydrodynamic stability theory as it applies in this context, that is, the investigation of the conditions under which small disturbances to the motion can grow. The logical development of the preceding chapters will be followed by restricting the discussion to dynamic instabilities due to shearing motions of a statically stable initial stratification. 'Convective' instability associated with an increase of density with height will be left until chapter 7, and two-component systems, in which different diffusivities play a vital role, will be treated separately in chapter 8.

The problem of instability of layers across which both density and velocity are rapidly varying functions of height is given special attention here, since such shear layers are very common in the atmosphere and ocean, and the vertical transports of properties such as heat and salt depend strongly on what happens near them. The topics covered now will, however, go beyond what is usually meant by the term 'instability' in the strict sense. It seems useful at the same time to outline other ways in which energy can be fed into limited regions of a more extensive flow, at a rate sufficient to cause a local breakdown. Some of the phenomena have already been mentioned in the context of steady flows, and the wider geophysical implications of the results will be discussed in chapter 10.

https://doi.org/10.1017/CBO9780511608827.005

4.1. The stability of a free shear layer

4.1.1. *The various types of instability*

We cannot do justice here to the extensive literature on hydrodynamic stability, or even to the small part of it which deals with stratified shear flows. Before considering special cases, however, it seems desirable to outline the methods used and to give a physical picture of the various possible mechanisms which can lead to instability. Details are to be found for example in the book by Betchov and Criminale (1967), and the review by Drazin and Howard (1966) (the latter concentrates specifically on the inviscid stratified case).

Consider first a homogeneous, inviscid two-dimensional flow in the x-direction, with velocity $u(z)$. If this has a wave-like disturbance with horizontal wavenumber k and phase velocity c imposed on it, then it follows from the equations of motion that the amplitude of a small vertical velocity perturbation w' can be described by

$$\frac{\mathrm{d}^2 w'}{\mathrm{d}z^2} = \left[(u-c)^{-1}\frac{\mathrm{d}^2 u}{\mathrm{d}z^2} + k^2\right] w'. \tag{4.1.1}$$

This equation, obtained by Rayleigh, has been extended by others to include the effects of viscosity and density gradients, through the addition of terms involving the Reynolds and Richardson numbers respectively. In the latter case, this adds a term $(u-c)^{-2}(\mathrm{d}u/\mathrm{d}z)^2 Ri$ to the square brackets on the right (where Ri is the gradient Richardson number defined by (1.4.3), and the Boussinesq approximation has been used). The equation poses in each case an eigenvalue problem, which allows one to determine for given boundary conditions a criterion for neutrally stable waves. This takes the form of a relation between k, the phase speed and the appropriate physical parameter (e.g. Re or Ri). It is also possible to calculate growthrates of the unstable disturbances as a function of these parameters, and numerical methods have been developed which now allow quite general flows to be investigated.

Let us turn now to the problem of particular interest, a density interface across which there is a velocity difference. Benjamin (1963) has distinguished three types of instability which can occur in this situation, and though his ideas were applied initially to the

motion of a fluid near a flexible solid boundary they are readily adapted to the two-fluid interface. What he has called Class A instability takes the form of waves which are of the same kind as Tollmien–Schlichting (T–S) waves, the mechanism of breakdown of flows near fixed solid boundaries. The presence of viscosity is essential for the growth of these waves. The disturbance originates at the critical level where $u = c$ (using the notation of (4.1.1)), but in order for this to grow, momentum must be transferred from the wall to the critical layer (by Reynolds stresses). A small but non-zero viscosity makes it possible to initiate this process in flows for which the inviscid solution is stable; the loss of energy by the mean flow exceeds the gain by the oscillatory motion. (A larger viscous effect can again lead to damping, and this of course is the origin of the critical Reynolds number criterion for transition to turbulence.)

Class B disturbances are related on the other hand to the free surface waves which can exist in the flexible medium when there is no flow over it. In the two-fluid context, they are like waves on the surface of the sea, and are the kind considered by Miles (1957) in his theory of wind-generated waves. (See also Lighthill (1962) for a physical interpretation of the mechanism.) The shear of the 'wind' profile is an essential factor for the growth of such waves: provided the curvature is negative at the critical height z_c, energy and momentum can be extracted from the mean flow at that level and transferred to the surface below. This mechanism is effective only for wavelengths very much longer than z_c, and dissipation acts now always to inhibit the growth. Care is necessary when trying to apply these ideas to 'internal' interfaces, since in the limit of small density differences which is of special concern to us here there is a range of velocities for which unstable waves are of Class A (i.e. viscosity becomes a destabilizing influence).

The Class C, or Kelvin–Helmholtz (K–H) instability, occurs when waves of the above two types (in the fluid and on the 'flexible boundary' or interface) coincide in both speed and wavelength. Historically this was the first kind to be described, and it will be discussed explicitly in §4.1.2. It leads to a violent breakdown at an interface and in a region on each side of it, whose character is practically independent of viscosity. It can be interpreted alternatively as a result of the action of the pressure disturbance in phase

with the interface elevation in overcoming the 'stiffness' of the surface (due to the restoring force of gravity in the case of interest here), and in terms of the instability of a vortex sheet (or more diffuse vortex layer).

The results quoted later suggest that the form of instability which is actually observed first on an interior shear layer in a stably stratified fluid is of the Kelvin–Helmholtz type, and that the breakdown can therefore be treated as an inviscid problem. Benjamin (1963) has shown that when the density difference is small, a Class A wave is the first which can theoretically become unstable, at a velocity difference across the interface of $(1/\sqrt{2})$ times that necessary for the K–H mechanism to operate; but the growthrate of the former is so much slower that it is overwhelmed by the latter in any situation where the shear continues to increase.

4.1.2. *The Kelvin–Helmholtz mechanism*

The results of inviscid stability analyses for various density and shear profiles will be considered in turn, beginning with the simplest case of a vortex sheet between two deep uniform layers moving with different velocities. This can be treated using the method described in §2.1 (and see Lamb (1932), p. 373 for the history of this problem) by defining the velocity potentials so as to include the mean flow as well as the disturbance. Using the same notation as before,

$$\phi_0 = -U_0 x + \phi_0', \quad \phi_1 = -U_1 x + \phi_1', \tag{4.1.2}$$

where U_0 and U_1 are the layer velocities in the positive x-direction.

A theorem due to Yih (1955) has shown that the first disturbances to go unstable as Ri is decreased are two-dimensional, so it can be assumed without loss of generality for the present purpose that the displacements are again of the form (2.1.2). Applying the conditions that the displacement and the pressure must be continuous across the interface, and eliminating a, A_0 and A_1 now leads to

$$\rho_0(\omega - kU_0)^2 + \rho_1(\omega - kU_1)^2 = gk(\rho_1 - \rho_0). \tag{4.1.3}$$

The phase velocity $c = \omega/k$ is

$$c = \frac{\omega}{k} = \frac{\rho_0 U_0 + \rho_1 U_1}{\rho_0 + \rho_1} \pm \left\{ \frac{g}{k}\frac{\rho_1 - \rho_0}{\rho_1 + \rho_0} - \frac{\rho_0 \rho_1}{(\rho_0 + \rho_1)^2}(U_1 - U_0)^2 \right\}^{\frac{1}{2}} \tag{4.1.4}$$

which reduces to (2.1.5) when $U_0 = U_1 = 0$. The first term is a weighted mean velocity of the layers, and the waves move relative to this with a phase speed related to the shear across the interface.

The stability of the interfacial waves depends on the character of the second term in (4.1.4). The square root is imaginary (so that the disturbances are exponentially growing and stationary relative to the mean velocity, rather than oscillatory) and the flow unstable if

$$(\Delta U)^2 = (U_1 - U_0)^2 > \frac{g}{k}\frac{\rho_1^2 - \rho_0^2}{\rho_0 \rho_1}. \qquad (4.1.5)$$

For a given velocity difference, the motion will be unstable and waves will grow if k is sufficiently large.† In the limiting case of zero density difference, *all* disturbances are unstable. This example illustrates a more general result: when the phase velocity of waves is expressed as a complex function $c = c_r + ic_i$, the magnitude of the imaginary part of the frequency kc_i is a measure of the growthrate, and the criterion for *marginal* stability is $c_i = 0$.

For comparison with later results we note that (4.1.5) can, in the case of a small density difference, be written as

$$\frac{(\Delta U)^2}{g'\lambda} > \frac{1}{\pi}, \qquad (4.1.6)$$

i.e. in the form of a critical internal Froude number (or inverse Richardson number) based on the wavelength of the disturbance. This indeed is the only form which can arise when buoyancy and inertia forces alone are acting and there is no other relevant length scale in the problem.

The result (4.1.3) can easily be generalized to give the condition that there should be stationary, neutrally stable waves ($c = 0$) on an interface between layers of finite thickness h_0 and h_1:

$$\rho_0 U_0^2 \coth kh_0 + \rho_1 U_1^2 \coth kh_1 = \frac{g}{k}(\rho_1 - \rho_0). \qquad (4.1.7)$$

In the limit of very long waves, this reduces to the form (3.2.17), quoted in the context of hydraulic theory. The limiting relation is not a stability criterion of the same kind as (4.1.5): even if it is satisfied,

† As in chapter 2, surface tension effects are neglected here; but surface tension would limit this instability by providing an extra restoring force which is important for small wavelengths.

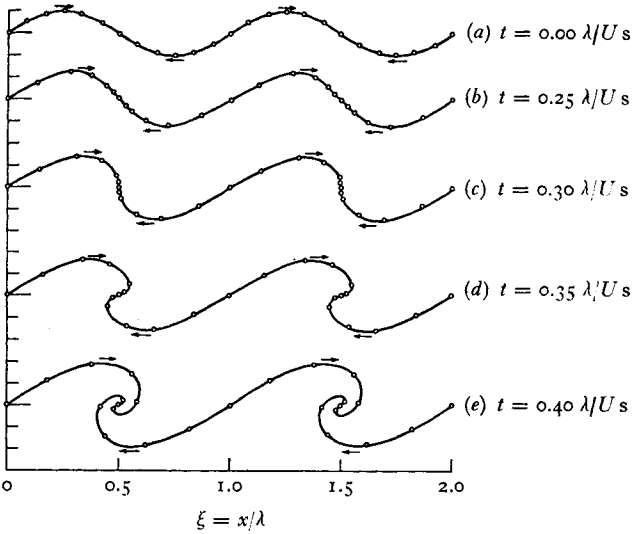

Fig. 4.1. The rolling up of a vortex sheet which has been given a small sinusoidal displacement. (From Rosenhead 1931.)

the flow may already be unstable to other disturbances of shorter wavelength. (It is related to the propagation rather than the growth of waves, and implies that a two-layer flow cannot be changed gradually through a state where (3.2.17) applies without leading to the violent disruption of the flow by an internal hydraulic jump.)

It must be emphasized again that the above results are based on *linear* theory, so that one can strictly obtain information only about the initial stages of growth, and cannot assume that the exponential growth will continue indefinitely (until the waves 'break' for example). In the limiting case of a vortex sheet with no density difference across it, however, Rosenhead (1931) made a calculation taking non-linear terms into account which should be valid at later times. The development of the shape of an originally sinusoidal interface is shown in fig. 4.1, which indicates that it winds up into a spiral form due to the interaction of the various parts of the vortex sheet and the distortion of the waveform by the mean flow. It will be seen later that patterns very like this are observed when a density interface becomes unstable.

4.1.3. *Interfaces of finite thickness*

Taylor (1931*a*) and Goldstein (1931) extended these calculations to more realistic shear and density distributions, using (4.1.1) with the term proportional to Ri added:

$$\frac{\mathrm{d}^2w'}{\mathrm{d}z^2} = \left[(u-c)^{-1}\frac{\mathrm{d}^2u}{\mathrm{d}z^2} + (u-c)^{-2}\left(\frac{\mathrm{d}u}{\mathrm{d}z}\right)^2 Ri + k^2\right]w'. \quad (4.1.8)$$

Again the effect of viscosity was not considered explicitly, only indirectly through its effect on the velocity distribution (whose form, as a function of z, will also be called the velocity profile). They discussed for simplicity a series of layers, in each of which Ri is zero or constant, and matched the conditions across the interfaces. The examples which are most relevant here are illustrated in fig. 4.2.

Case (*a*) is a layer of intermediate density and thickness h between two deep uniform layers, with the velocity changing linearly between constant values over this same depth. If an overall Richardson number is defined using the total density and velocity changes and the lengthscale h, $Ri_0 = g(\Delta\rho/\rho)h/(\Delta U)^2$, then the boundaries of the unstable region are as shown in fig. 4.3, which is a plot of Ri_0 against non-dimensional wavenumber $\alpha = \frac{1}{2}kh$. In contrast with the result (4.1.5) for the vortex sheet, the distribution of the vorticity over a finite depth h has stabilized the higher wavenumbers, and only disturbances in a narrow band of intermediate scales are unstable. The unstable range is centred on the state where the waves on both interfaces move with the same velocity, and it becomes narrower at higher values of Ri_0.

The second case (*b*) has the same linear velocity change but a continuous exponential density variation through the intermediate layer (which is also effectively linear in the Boussinesq approximation). Goldstein's approximate calculation has been clarified and extended by Miles and Howard (1964), whose stability diagram is drawn in fig. 4.4, using the same variables as in the previous case. At low Ri_0 (which is now also the gradient Ri through the interface) there is again a range of intermediate wavenumbers which are unstable. The significant new point is that above $Ri = \frac{1}{4}$ small

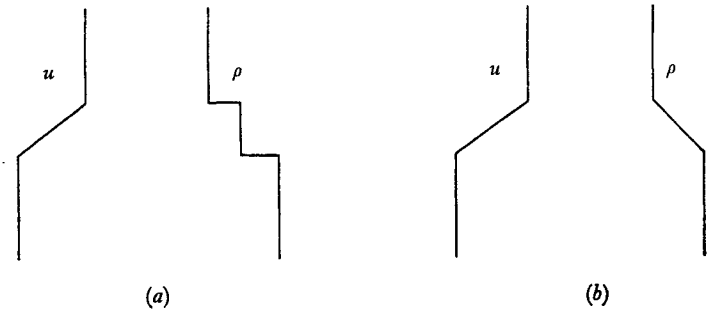

Fig. 4.2. Velocity and density profiles used in the first interfacial stability calculations.

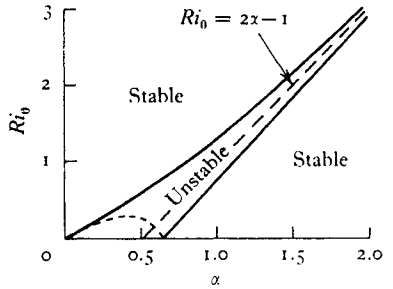

Fig. 4.3. The stability characteristics of a shear layer corresponding to fig. 4.2*a*. Waves which can grow on the density discontinuities contribute significantly to the instability.

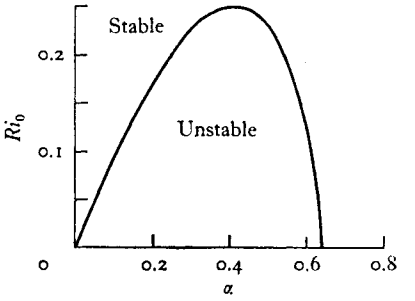

Fig. 4.4. The stability characteristics of a shear layer corresponding to fig. 4.2*b*. Note the difference in scales, and the very much smaller region of instability compared to fig. 4.3. (The stability boundary in fig. 4.4 has been added to 4.3 for comparison, as the dotted line.)

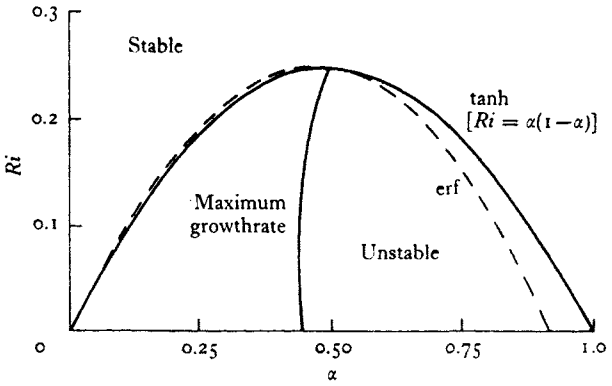

Fig. 4.5. The stability boundaries and wavenumbers for maximum growthrate for interfaces with tanh and error function profiles of both velocity and density. (After Hazel 1972.)

disturbances of *all* wavenumbers are stable.† The 'most unstable' wave, defined as the first to go unstable as Ri is reduced below $\frac{1}{4}$, is given by $kh = 0{\cdot}83$, i.e. it has a wavelength

$$\lambda = 2\pi/k = 7{\cdot}5h, \tag{4.1.9}$$

and it travels with the mean velocity of the layers. Miles and Howard also calculated growthrates in the unstable range.

Using mostly numerical methods, calculations have now been carried out for a variety of smoothly varying profiles of both density and velocity. Drazin (1958) assumed an exponential density variation and a tanh velocity profile, and showed that the critical Ri, above which all small disturbances are stable, is again $\frac{1}{4}$, and occurs at $kh = \sqrt{2}$ (where Ri and h are now based on the gradients at the centre and the total velocity change). The use of similar tanh profiles for both density and velocity gives a parabolic boundary of the unstable region, with $Ri = \frac{1}{2}kh(1 - \frac{1}{2}kh)$, and the most unstable wavenumber is at $kh = 1$. Hazel (1972) has shown that this last result is not sensitive to the exact form of the distributions (it is little changed when error function profiles are used), and his computations of the stability boundaries and maximum growthrates for lower values of Ri are shown in fig. 4.5. The most unstable wave-

† This is a context in which the use of a 'gradient Froude number' $F_g = Ri^{-\frac{1}{2}}$ would be an advantage, so that large values of F_g correspond to instability; current usage decrees otherwise, and we continue to use Ri here.

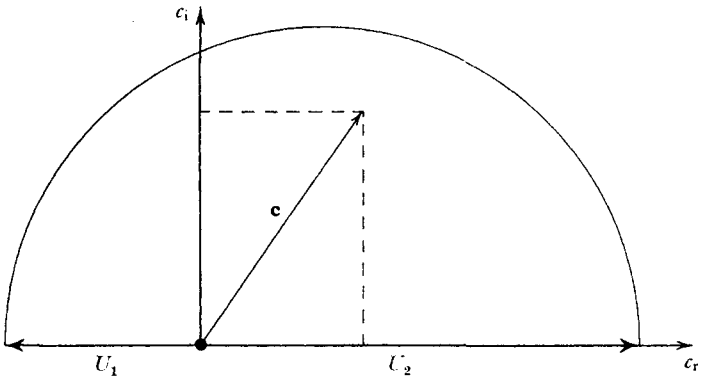

Fig. 4.6. Howard's 'semi-circle theorem', summarizing the conditions on the complex wave velocity which must hold if disturbances are to grow on an interface.

length can vary with the profiles chosen, but its range (from the value given in (4.1.9) to $\lambda = 2\pi h = 6.3h$ for the smoothly varying profiles) is small for distributions which represent the kind of interface which is of most interest here.

Various general criteria for instability have also been obtained from the stability equation without reference to particular profiles. For a detailed account of these see Miles (1961, 1963) and the review by Drazin and Howard (1966, p. 60), but three results will be mentioned here. Rayleigh's result for homogeneous inviscid fluids, which states that there must be a point of inflexion in the velocity profiles for instability to occur, has been generalized. The form with stratification is not so useful (nor so simple), since it involves the unknown wave velocity c, and it is not known if an inflexion point is necessary. Secondly, Howard (1961) showed that the complex wave velocity for any unstable disturbance must lie inside the semi-circle in the upper half of the complex plane which has the total range of velocities (i.e. the velocity of the upper and lower layers far from the interface) as diameter (see fig. 4.6). This sums up a number of earlier results which put limits on the wave velocity and growth-rates, and it can considerably simplify numerical calculations. The simplest and most readily applied condition is that of Miles (1961), which states that the *sufficient* condition for an inviscid continuously stratified flow to be *stable* to small disturbances is that $Ri > \frac{1}{4}$ everywhere in the flow.

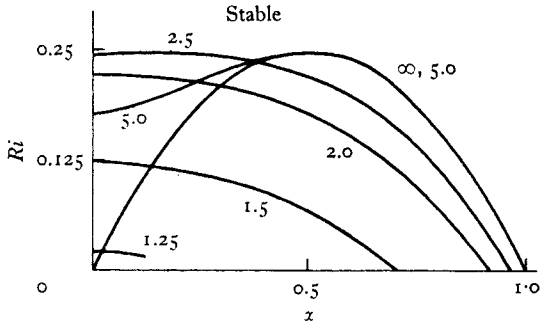

Fig. 4.7. The effect of horizontal boundaries on the stability of a density interface to a shear (after Hazel 1972). The numbers against the curves are the ratios of the total depth to a characteristic thickness of an interface with tanh profiles of density and velocity.

We should note particularly the wording of the last result; it does *not* imply that the flow must become unstable if Ri falls below $\frac{1}{4}$ somewhere, as one might be tempted to say on looking at the particular cases shown in figs. 4.4 and 4.5. Counter examples have been found; for instance, with a jet-like velocity profile $u \propto \operatorname{sech}^2 z$ and an exponential density profile, the flow can become unstable if $Ri_{\min} < 0.214$, somewhat less than the Miles limit. Hazel (1972) has shown too that rigid boundaries can have a stabilizing influence. The change in the stability boundaries for a flow with tanh profiles is shown in fig. 4.7, as symmetrically placed horizontal walls above and below are moved in from infinity. (The numbers against the curves represent the ratio of the depth of the region to the thickness of the transition layer.) The first, and very surprising, effect is to make long waves less stable, but at smaller separations all wavenumbers are stabilized. The lesson to be learnt here is that the whole profile matters in determining the 'critical Richardson number'.

The stability also varies considerably when the profiles in the transition region are assumed to have the same shape but different thickness. For example Hazel considered the case $u = \tanh z$, $\rho = \tanh(rz)/r$, and showed that the stability depends strongly on the factor r. The variation of gradient Richardson number with height is shown in fig. 4.8 for various values of r; for $r < \sqrt{2}$ (and so certainly for all cases $r < 1$ where the density interface is wider than the shear) the minimum Ri occurs at the centre, and there is insta-

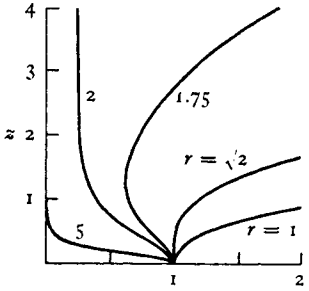

Fig. 4.8. The variation of gradient Richardson number with height as a function of the ratio r (the ratio of velocity to density interface thickness).

bility when $Ri < \frac{1}{4}$. For $\sqrt{2} < r < 2$ the minimum value is smaller and displaced from the centre, and disturbances at these points will grow fastest. At even higher values of r where the density profile is very thin compared to the shear no critical value of Ri is relevant and the behaviour is more nearly like that considered in §4.1.2.

Many interesting problems remain to be investigated in this field. It would be useful, for example, to have results for flows with boundaries unsymmetrically placed with respect to the density profile (see §4.2.3).

4.1.4. *Observations of the breakdown of parallel stratified flows*

The predictions of the above theory have been tested in several recent laboratory experiments. Scotti and Corcos (1969) made measurements in a carefully designed wind tunnel, in which they set up a two-layer flow stratified with temperature (taking precautions to avoid heating and cooling effects at the walls). They worked always at large enough velocities for the flow through the entry section to be supercritical in the sense implied by (3.2.18), so that all disturbances were swept downstream. A small shear across the interface was generated because the lighter air stream was accelerated more than the heavier by the imposed pressure gradient through the contraction, and this shear then remained constant downstream. The interface thickened downstream due to diffusion of heat and vorticity, but the profiles of Ri remained similar: the distribution must be like that shown in fig. 4.8 for low r, with a minimum at the centre (the approximate r in air is about 0.8, since

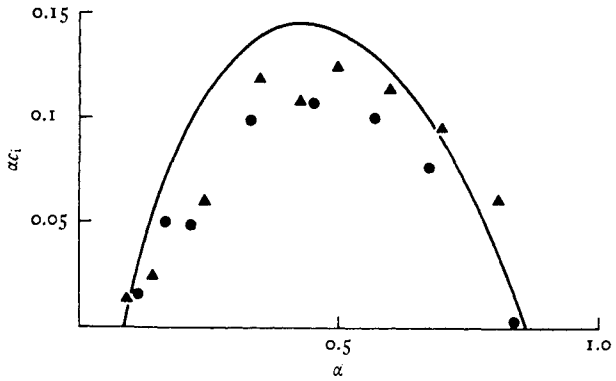

Fig. 4.9. Comparison of measurements of waves on a sheared interface with the predictions of inviscid theory. Minimum $Ri = 0.07$; the symbols denote two experimental runs, and the line represents the computed growthrates. (From Hazel 1972.)

the temperature profile spreads faster than the velocity). A slight adjustment of the depth of the tunnel allowed Ri to be kept nearly constant throughout the length of the working section and for a long time.

Very small waves were generated using a thin wire oscillated with controlled frequency at the centre of the interface, and their growthrate (in time) measured by observing the change in amplitude down the tunnel. When $Ri_{\min} < \frac{1}{4}$ the waves grew at a rate which depended on $Ri_{\min}$ and wavenumber, and when $Ri > \frac{1}{4}$ they were attenuated, the decay rate being independent of Ri. The measured growthrates at $Ri_{\min} = 0.07$, for example, are compared in fig. 4.9 with Hazel's (1972) calculation for the same profiles, based on inviscid theory. The agreement is good, and the waves travelled with the mean flow in accordance with the theoretical prediction.

The experiment of Thorpe (1968*b*, 1971) has already been referred to in passing in §§2.3.3 and 3.2.4. He produced a shear flow in a stratified fluid contained in a closed tube of rectangular section, by tilting the tube away from the horizontal. The velocity profiles generated as gravity accelerates the flow are closely linked to the density distribution, and can be calculated from it using inviscid theory or with viscous corrections added. Until the surges formed at the ends of the channel reach the centre, the flow is parallel, and this is therefore a very useful experimental configuration. Observa-

tions of stability can be compared with theory which has been extended to allow for the acceleration. Experiments have been carried out also with linear salinity gradients (in this case no instability was observed although Ri fell as low as 0.014) and immiscible fluids (Thorpe 1969*b*) but only the case of two miscible layers will be discussed in any detail here.

Two layers, a layer of fresh water above a salt solution, were put into the tube while its long axis was nearly vertical. It was then brought carefully to a horizontal position and the interface allowed to spread by diffusion for a known time (so that the density distribution through it could be calculated). The tube was tilted again rapidly through a small angle and left there, and after a few seconds a regular array of waves suddenly appeared on the interface. These waves were stationary when the layer depths were equal, and grew; in about a second they rolled up (as shown in the photographs in fig. 4.10 pl. VIII) into a form closely resembling that of fig. 4.1. The wavelengths, and the velocity difference at which the waves appeared, were in good accord with theory applicable to an accelerating flow. Thorpe also showed that, though viscosity affected the velocity profile in some of his runs, fair agreement with the measured growthrates was obtained by treating these profiles using the inviscid theory, i.e. no damping effect of viscosity was apparent down to Reynolds numbers (based on the maximum shear and the momentum thickness of the shear region) of about 100. This conclusion is supported by the more recent stability calculations of Maslowe and Thompson (1971).

At later times, the interfacial rolls break up completely to produce a thickened interface (Thorpe 1971). Visual observations suggest that this consists of a relatively well-mixed interior bounded by sharp gradients at the edges (as sketched in fig. 4.11, and shown in the sequence of shadowgraph pictures in fig. 4.12 pl. VIII). Detailed measurements of concentration profiles (Thorpe, personal communication) indicate, however, that the final mean density gradient is more nearly linear through this thickened interface, with many small scale steps and interfaces superimposed on it, rather than two large steps at the edges as was first supposed. (For further discussion related to this interfacial structure, see §§4.3.1, 5.3.2 and 10.3.1.)

When the original layers are deep and their velocity is held

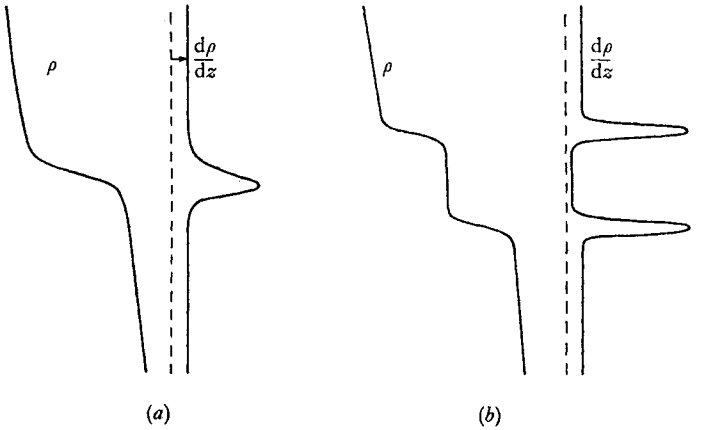

Fig. 4.11. Sketch of the assumed density and density gradient profiles, (*a*) before and (*b*) after mixing produced by the K–H instability.

constant after the instability is observed (by returning the tube to the horizontal), an energy argument (cf. §10.2.3) shows that the growth of the interface will be limited and the layers remain distinct. If the flow continues to be accelerated, a new instability can arise on the thickened interface (see §5.3.2). When the layers are not deep compared to the thickened interface, the rolls fill the whole of the channel, and turbulence generated at the solid boundaries will also help to mix both layers thoroughly together.

In subsequent sections we will need to distinguish carefully between instabilities (and mixing) driven by processes occurring at the interface itself, and those due to turbulence produced by some other mechanism elsewhere in the flow. By keeping this difference in mind now, one can explain another observation reported by Thorpe. If, during the setting up of the experiments just described, the axis of the channel was tilted *suddenly* from vertical to horizontal, the equivalent of the 'lock exchange' flow (§3.2.4) was set up, with two 'noses' advancing along the tube in opposite directions. At no time were large overturning instabilities observed on the interface in this case, but instead smaller, less regular travelling disturbances appear, having the cusp-like form shown in fig. 4.13 pl. IX. These are very like the forced waves produced by turbulent stirring in the layers (see chapter 9), and the difference in behaviour can be interpreted as follows.

In the first case, with accelerating laminar layers, the density and velocity gradients are sharp and both confined to an interface of thickness h. The interfacial (gradient) Ri is smaller than the overall Ri_0 based on the layer depth H and related to it by

$$Ri \approx \frac{h}{H} Ri_0. \tag{4.1.10}$$

Not only is $h/H < 1$ in this situation, but Ri_0 may be made small by waiting long enough, and so Ri will eventually fall below the critical value. If, on the other hand, the velocity profile is determined independently of the sharpness of the density step (as is likely in the steady turbulent counter flows well behind the 'noses'), it will have a lengthscale more nearly comparable with H, so that

$$Ri \approx \frac{H}{h} Ri_0. \tag{4.1.11}$$

It has been shown (3.2.13) that in this latter case $Ri_0 = \frac{1}{2}$ in a horizontal channel, so whatever the value of $H/h > 1$, no instability of the K–H type is to be expected (but remember fig. 4.8).

A laboratory observation which at first sight contradicts the above statement has been made by Simpson (1969); he showed that K–H 'billows' can form immediately behind the front of a gravity current (§3.2.5). In that case, however, the velocity gradient in the non-turbulent accelerating flow over the nose must again be determined by the density gradient, and a small gradient Ri can be obtained.

Several striking atmospheric phenomena can be understood in terms of the instability of a steady parallel shear across a region of strong temperature gradient. Some kinds of billow clouds certainly arise in this way; Ludlam (1967) has documented some good examples, one of which is reproduced in fig. 4.14 pl. x. Recently high power radar techniques have been used in conjunction with vertical soundings of wind and temperature to document the onset of K–H instabilities even when there is no cloud. Atlas *et al.* (1970), for example, have obtained echoes from a thin layer of high temperature gradient but small Ri, and have followed billows as they grow, overturn and finally break down to leave a patch of 'clear air turbulence' (fig. 4.15 pl. ix). The original single sharp radar echo is

split into two, and this structure has been explained in terms of larger gradients at the edge of the turbulent layer, just as in the laboratory experiments (figs. 4.11 and 4.12).

The formation of billows is often associated with internal waves, which can produce quasi-steady shears on density interfaces. For many purposes these are locally equivalent to the steady shear described above, but they will be discussed separately in §4.3.3.

4.2. The combined effects of viscosity and stratification

Much less is known about the stability of flows in which both viscosity and buoyancy as well as inertia forces are important (but see Drazin (1962) for a general survey of the whole range of possible problems). One difficulty is that sometimes viscosity has been invoked explicitly when an alternative explanation can be given with viscosity playing only a secondary role. Several problems of this kind are included below, as well as one in which viscous effects enter more directly.

4.2.1. *Viscous effects at an interface*

Thorpe's experiments (§4.1.4) have made it clear that the stability of a density interface is well described by inviscid theory, even when the velocity profile is influenced by viscosity. The only likely exception to this rule in an unbounded fluid is a flow at very low Reynolds number, where viscous damping will then reduce the growthrate of disturbances. (See Betchov and Criminale 1967, p. 79.) Much earlier, however, Keulegan (1949) carried out an extensive and much quoted series of experiments, using a pool of sugar solution with a laminar or turbulent flow of fresh water above it. He invoked viscosity to interpret his results, but they should now be re-examined in the light of the more recent work.

Keulegan's essential result can be obtained using dimensional reasoning. Given a velocity U (the mean velocity of the upper layer), a density difference or $g' = g\Delta\rho/\rho$ and the kinematic viscosity ν (of the lower fluid), only one non-dimensional parameter,

$$K = U^3/\nu g', \tag{4.2.1}$$

can be formed. With a laminar flow, the onset of instability (as judged by the appearance of waves on the interface) was shown to depend mainly on K, and occurred at a critical value of about $K = 500$.

Now let us substitute for ν in (4.2.1) using the viscous lengthscale $d = (\nu x/U)^{\frac{1}{2}}$ (the thickness of the boundary layer formed in time x/U as the flow travels a distance x from the entrance of the channel) to obtain

$$K = \frac{U^2}{g'd}\left(\frac{xU}{\nu}\right)^{\frac{1}{2}}. \tag{4.2.2}$$

This criterion for instability can therefore be thought of as a Richardson number condition based on the depth of the shear layer, with an additional weak dependence on a Reynolds number Re. With this experimental arrangement the velocity profile is determined completely by the diffusion of vorticity and is not linked to the density profile (as it is in the tilted channel). Since the density distribution was not measured, a quantitative comparison of the two ideas is not possible in retrospect; but the range of mean velocities and hence Re used was small and a completely inviscid explanation of the instability now seems more likely than the original one.

In the turbulent case, Keulegan observed some disturbance of the interface at all velocities (cf. figs. 4.13), and defined 'instability' as the point where the rate of mixing suddenly increased (due to the formation of larger scale K–H waves). This occurred at a lower constant value of $K = 180$, presumably because of the sharpening of the gradients through the interface at a given mean velocity. This is again consistent with an inviscid interpretation, but it is at first sight contrary to the explanation given in §4.1.4 of the contrast between the photographs of figs. 4.10 and 4.13. It must be remembered, however, that the velocity profiles in the two laminar experiments are produced in quite different ways, and are likely to be sharper when the motion is driven by buoyancy differences across a sharp interface.

4.2.2. *Thermally stratified plane Poiseuille flow*

Definite theoretical results have been obtained for a class of plane viscous flows, the most important example being a parabolic

velocity profile between solid walls maintained at different temperatures (so that there is a conductive heat flux through the walls and the undisturbed temperature gradient is linear). In this case both viscosity and also the diffusivity of the property determining the density (e.g. heat) are genuinely important in the stability problem. The limiting case of a destabilizing density gradient and zero velocity will be discussed separately in chapter 7. Here we present some of the results for the combined problem, emphasizing the case where the density distribution is heavy at the bottom.

This flow can be defined in terms of three non-dimensional parameters formed from the maximum velocity U_*, the depth d, the density difference $\Delta\rho$ between the bottom and top walls, and the molecular properties ν and κ. Following the original development of Gage and Reid (1968) (and setting aside for the moment the extension to other profiles due to Gage (1971)) we use

$$Re = \frac{U_* d}{2\nu}, \quad Ra = -\frac{g(\Delta\rho/\rho)\, d^3}{\kappa\nu}, \quad Ri = \frac{g(\Delta\rho/\rho)\, d}{16 U_*^{\,2}} \qquad (4.2.3)$$

i.e. a Reynolds number, a Rayleigh number (see § 3.3.4 and chapter 7), and an overall Richardson number which corresponds exactly to the gradient Richardson number near the wall. (For a fixed value of $Pr = \nu/\kappa$, taken by Gage and Reid to be unity in their numerical calculation, Ra and Ri are alternative parameters, not independent ones.) When the density difference is destabilizing (Ra positive), there are two kinds of instability. The first is purely 'thermal' in origin; it sets in at a value of Ra which is independent of the shear and takes the form of rolls with axes in the direction of mean flow. The other leads to the Tollmien–Schlichting type waves characteristic of a shear flow instability over a solid boundary. There is an abrupt transition between the two at about $Ri \approx -10^{-6}$, the thermal instability dominating at larger values of $|Ri|$; the smallness of this number emphasizes the dominant role of the density gradient.

When Ri is positive (and the stratification stabilizing) Gage and Reid again found numerically the form of the stability curves, plotting wavenumber against Re for various fixed values of Ri. With $Ri = 0$ there is an unstable loop in the k, Re plane, the minimum of which gives the critical value of Re. As Ri is increased, the

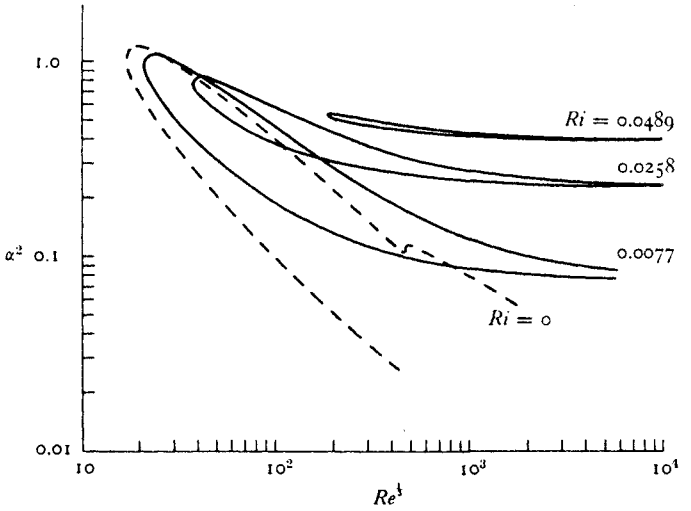

Fig. 4.16. The neutral stability curves (Reynolds number Re as a function of non-dimensional wavenumber α) for various values of Richardson number in stably stratified plane Poiseuille flow. (After Gage and Reid 1968.)

area of the loop decreases (see fig. 4.16) and the critical value Re_{crit} increases. The theory thus predicts that above $Ri = 0.0554$ the flow will be stable to small disturbances no matter how large is Re. It also shows that with any smaller Ri the flow is stable if Re is sufficiently small, and at large Re the instability is confined to a particular narrow range of wavenumbers. Extending the arguments to velocity profiles with inflexion points, Gage (1971) has shown that this conclusion is not changed qualitatively, though the numerical values are different. For a particular profile he showed that complete stabilization is still achieved, at a Richardson number (evaluated at the critical point) of about 0.107.

The much smaller value of the critical Richardson number obtained here (compared to that for a free shear layer) suggests that a boundary always has a stabilizing influence, in spite of the viscous mechanism for instability which it introduces. (The stabilizing effect of symmetrical boundaries on an inviscid interface has already been shown in fig. 4.7.) A similar deduction was made much earlier by Schlichting (1935), though his theory was less satisfactory since it neglected diffusion. He applied his results to the discussion of the boundary layer under the heated roof of a wind tunnel, which

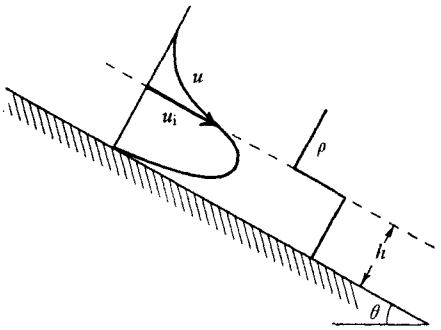

Fig. 4.17. Definition sketch for the flow of a heavy layer down a slope.

was observed to remain laminar up to high Reynolds numbers provided $Ri > \frac{1}{20}$.

When comparing these results with those treated later we must keep clearly in mind the two features which distinguish the problem discussed in this section. There must be a constraining effect, as provided here by the solid boundary (but perhaps a region of much stronger stability could behave like a wall for this purpose). Secondly, the stable density gradient must continue right down to this 'wall', which is only possible when there is a flux of buoyancy through it. (See §4.3.1.)

4.2.3. *Flows along a sloping boundary*

Another case where the role of viscosity is ambiguous is the flow of a gravity current along a sloping boundary. This has been discussed in §3.2.3 (using hydraulic theory) and will be mentioned again in §6.2 (where mixing is of prime concern), but here we investigate the stability of the laminar flow. In addition to being driven by the component of gravity acting down the slope, this will be subject to a stabilizing component across the flow and therefore is related to the other problems treated in this section. We first summarize the properties of the *steady* flow of a uniform layer of heavy viscous fluid flowing under a lighter fluid (sketched in fig. 4.17), whose stability is to be investigated.

Integration of the viscous equation of motion through the depth h of the lower layer leads to

$$u = \frac{g' \sin\theta}{2\nu}[zh - z^2] + u_1 \frac{z}{h}, \qquad (4.2.4)$$

where $u(z)$ is the velocity parallel to the slope and u_1 is the velocity of the interface. In terms of the mean velocity $\bar{u}$ through the layer this may be written

$$\frac{u_1}{\bar{u}} = 2 - \frac{1}{6}\frac{g' \sin\theta \cdot h^2}{\bar{u}\nu} = 2 - \tfrac{1}{6}H. \tag{4.2.5}$$

The dimensionless parameter H (the inverse of the J defined by Ippen and Harleman (1952)) can be written variously as

$$H = Re \sin\theta / F^2 = Re \cdot Ri_0 \tan\theta, \tag{4.2.6}$$

where

$$Re = \frac{\bar{u}h}{\nu}, \quad F = \bar{u}/(g'h)^{\frac{1}{2}} \quad \text{and} \quad Ri_0 = g'h\cos\theta/\bar{u}^2$$

(the overall Richardson number Ri_0 being defined to conform with §6.2, with the slope θ included in its definition). The numerical value of H can range from 3 for a free surface flow, to 12 when there is a fixed boundary at $z = h$. Ippen and Harleman found experimentally that $H = 7.3$ for the case of interest here, corresponding to $u_1/\bar{u}$ of about 0.59. This agrees with a theoretical result of Lock (1951) who showed that the overlying fluid is dragged forward by the layer to this extent. The important point is that H has a fixed value, so although both Re and F (or Ri_0) enter the problem, in fact only one of them can be chosen independently when the slope is given, the other being related to it through (4.2.6).

The different parameters used in the literature to describe the relative importance of buoyancy and viscosity can all be regarded as combinations of Re and F, and which is most appropriate depends on the boundary conditions. If, as here, some lengthscale is basic and the velocity is produced by buoyancy, then the Grashof number

$$Gr = \frac{g'h^3}{\nu^2} = Re^2/F^2 \tag{4.2.7}$$

should be chosen, since this retains h but removes $\bar{u}$. When the velocity difference across an interface is imposed and no external lengthscales are relevant then the parameter $K = \bar{u}^3/\nu g' = Re \cdot F^2$ used by Keulegan is appropriate (see §4.2.1). Thus it seems logical to use Gr to describe laminar flows driven along a slope by gravity, always bearing in mind that the use of a relation like (4.2.6) will convert it to an equivalent value of either Re or F alone.

Few definite theoretical results are available for the stability of these flows, though we can with some confidence make a generalization from the corresponding free surface cases (see Yih 1965 and Lin 1969). The stability boundary will be expressible as a relation between wavenumber k, slope θ and only one of Re or F (because of the relation between these, established above), and there will always be a minimum Re (or F) above which the flow becomes unstable. The experiments of Ippen and Harleman (1952) suggest that the two-layer flow always becomes unstable when $F = 1$, in the sense that the first wave-like disturbances appear then, with wavelength $\lambda \approx 3h$. This result was independent of slope (and therefore of Re) up to about $\theta = 9°$, and it implies that the breakdown is one which involves interfacial waves on the top of the layer, i.e. it is determined by the inviscid hydraulic criterion discussed in §3.2 and §4.1.2. (Compare with (4.1.6).) Sustained turbulence, on the other hand, was only observed when Re rose above about 1000, and so this must be associated still with the growth of T–S waves at the solid boundary.

It is instructive to compare this layer flow with the related case of a laminar boundary layer under a heated sloping plane in air, which has a continuous stable density profile right to the wall. (This, and its stability, will be described for a vertical wall and for inclined flows *above* the heated plate in §7.4, in the context of convective motion.) It suffices to say now that for a fixed $Pr = \nu/\kappa$, the flow can again be specified by a single parameter, usually taken as $Gr \sin\theta$ where the Grashof number Gr is based on the distance along the plate, but again equivalent to Re through a relation like (4.2.6). Tritton (1963) showed experimentally that for a range of large slopes between 40° and 90° from the horizontal, fluctuations first appear when Gr reaches a value which is nearly independent of the slope and which corresponds to a local value of Re (based on the volume flux) of about 250. He also carefully distinguished this first instability from the fully turbulent state, and both sets of results are shown in fig. 4.18, where critical values of $(Gr)^{\frac{1}{3}}$ are plotted against the angle θ to the horizontal. While the first instability is insensitive to slope, the attainment of the fully turbulent flow is definitely retarded by the stabilizing effect of the density gradient as the plane is tilted towards the horizontal. This is therefore another example

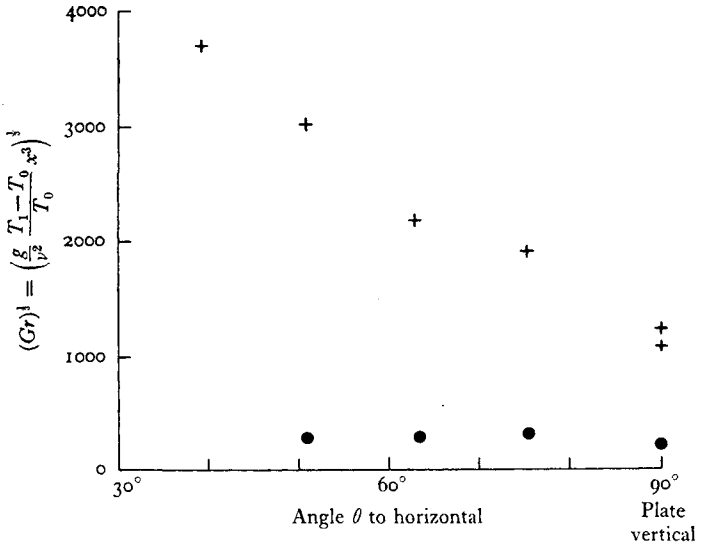

Fig. 4.18. Flow under a heated sloping plate: critical Grashof numbers corresponding to: ● first fluctuations and + fully turbulent flow at various slopes. (After Tritton 1963.)

of the kind of flow considered in §4.2.2, in which the gradient right up to the wall is important.

4.2.4. *Transition to turbulence*

Before leaving the subject of hydrodynamic stability as such, it is important to be clear about the relevance of the criteria it produces to the question of whether or not a given flow will be turbulent. The answer is already implied by the results of earlier sections, but some further discussion will emphasize the point. Linear stability theory only gives information about the initial growth of small disturbances, and can say nothing about their development at larger amplitude. Drazin (1970) has extended the calculations of the K–H instability into the slightly supercritical range, but no such theory can provide a reliable guide to the detailed behaviour under highly supercritical conditions. The most that can be said then is that the non-linear superposition of many unstable modes produces a truly turbulent motion.

Special care is needed when several physical parameters are

relevant. For layer flows at large slopes, (4.2.6) shows that the criterion $F = 1$ governing the appearance of the first wave-like instability will be satisfied at quite small values of Re. At such values, however, the effect of viscosity on the growth of disturbances can still be large, and a fully turbulent flow is not observed until Re is much greater, comparable with that required for turbulent pipe flow. When there is a density gradient sustained right to the wall, it is clear from Tritton's results (and the theory of §4.2.2) that the Reynolds number for transition to turbulence depends on Ri; but at small enough Re it is this parameter, not the buoyancy parameters Ri or F, which determine the point of transition.

It will be more generally true that the transition to turbulence will be a function of both Re and F, and that only when Re is sufficiently large can its effects be ignored entirely. Based on the experience with flows near boundaries one might suppose that decreasing either Re or F should always increase the stability, but very little is known about the critical values for other boundary conditions, for instance an intruding fluid layer bounded above and below by density interfaces. (Caution is suggested by the results of Thorpe (1969*a*), who showed theoretically that a certain stratified flow is unstable whereas the corresponding homogeneous (inviscid) shear flow is stable, and Hinwood (1967), who reported experiments which indicated transition in a pipe flow at lower Re with stratification than without.) In chapter 10 it is shown that the important limitation on turbulence at internal shear layers in a large body of stratified fluid (such as the ocean) may often be one of Reynolds number, but with the relevant vertical lengthscale set by the stable stratification.

Finally, it is worth remarking again that the basic property of a stably stratified fluid is its ability to sustain internal wave motions. These need not be unstable, and can certainly exist without there being any breakdown to turbulence. On the other hand, when the motion can be described as turbulent, in the sense that mixing and an enhanced rate of diffusion are observed, it is rarely possible to neglect wave motions entirely. Though these two aspects of a turbulent stratified flow will be considered separately in some of the following sections, the interaction between them must always be kept in mind, and this will be taken up again explicitly in the final chapter.

4.3. Mechanisms for the generation of turbulence

We now turn to the wider question of turbulent flows which are beyond any condition of marginal stability, and identify and compare the processes whereby turbulence and mixing can be produced in a stably stratified fluid. The source of energy for the maintenance of the turbulence must always be examined carefully: it seems fundamental to distinguish clearly between turbulence generated directly at a boundary, and that arising in the interior in various ways. A systematic classification can be based on this principle, and for convenience of later reference, the range of possibilities will first be described in general terms in §4.3.1. The detailed discussion of some of these cases must be deferred to later chapters, but we will follow up here several special problems which arise from topics which have already been introduced.

4.3.1. *Classification of the various mechanisms*

At the two extremes, it is easy to say whether the energy which is producing turbulence comes from an 'external' or 'internal' process. The mixing of a nearly homogeneous fluid flowing through a pipe or channel is determined entirely by boundary generated turbulence, and the mixing is carried out by eddies extending right across the flow (as shown diagrammatically in fig. 4.19*a*). At a density interface well away from boundaries (fig. 4.19*b*), across which a steady shear is established, the breakdown and the production of turbulence are certainly internal processes (§4.1.4), and the turbulent motions are confined to the interfacial region.

A special case of internal mixing will be identified in §5.1.4; it will be shown that the shear and density distributions can be maintained in a kind of marginally stable state, the turbulence being self-regulated by the mixing it produces. The outer edge of a turbulent gravity current flowing down a steep slope can be described in these terms (§6.2.3), since the scale of the turbulence is so strongly limited by the vertical density gradient that this region is effectively isolated from the boundary (fig. 4.19*c*).

The interpretation of other situations requires more care. Paradoxically, the very stable case of a thin, heavy layer flowing along

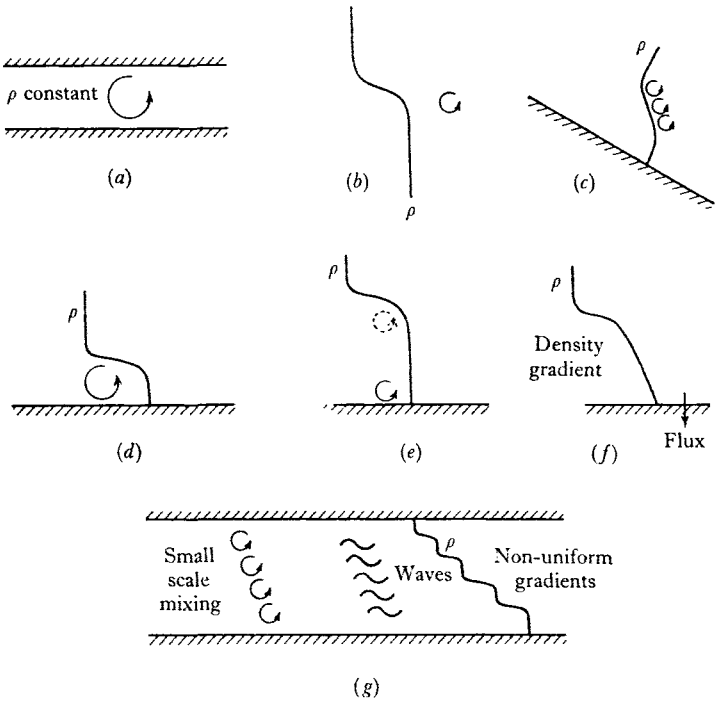

Fig. 4.19. Classification of mixing processes. (*a*) External mixing of homogeneous flow in a channel. (*b*) Internal mixing across a density interface remote from boundaries. (*c*) Self-regulated ('internal') mixing at the outer edge of a gravity current on a steep slope. (*d*) Gravity current on small slope: mixing across interface is driven by turbulence generated at boundary. (*e*) Small scale turbulence decays with distance from source. (*f*) Buoyancy flux also makes externally-generated turbulence ineffective at interface. (*g*) In strongly stratified channel flows the density gradient must be non-uniform, and both wave motion and turbulence will be important.

a horizontal boundary under lighter fluid (fig. 4.19*d*) has many features in common with the unstratified case (*a*). The mixing and stress across the interface are now very small (see §6.2) so that such a layer will be practically homogeneous and stirred by turbulence generated at the boundary. The mixing of fluid across the interface can then be regarded as a consequence of this turbulence, i.e. as a boundary-driven mixing process. This idea can be applied to layers which are stirred in other ways (see §9.1).

There are two circumstances in which turbulence produced at a solid boundary will become less effective in mixing across a density

interface some distance away. If, instead of being generated on the scale of the whole layer (as implied in (*d*)), the turbulence has a much smaller scale than this depth (fig. 4.19*e*), viscous dissipation will cause the turbulent energy to decay with distance from the source region. When the boundary-interface distance becomes large, this contribution to the energy will have a negligible effect on the interface compared with local processes, and we approach case (*b*) again. Secondly, when there is a buoyancy flux through the boundary in the sense which will produce a stable density gradient in the otherwise homogeneous layer (fig. 4.19*f*), all the turbulent energy made available at the boundary may be used in working against gravity in this region, leaving none for mixing across the sharper interface beyond.

On the other hand the boundary stress can remain an important parameter in channel flows having a substantial density gradient (and a large overall Richardson number), although one might at first sight expect these to be 'internally' limited. As discussed more fully in chapter 10, this can be so because such flows must be intermittently turbulent, part of the stress being carried by turbulence and part by waves (fig. 4.19*g*). In one sense the mixing is an interior process (because the turbulent motions will be limited in vertical extent, as in (*c*)). However, the whole of the vertical flux of horizontal momentum comes ultimately from the boundary, and this will continue to have an indirect effect on the interior turbulence, operating through the wave contribution to the momentum transport.

4.3.2. *Flows near boundaries*

It is obvious from fig. 4.19 that one cannot rely on the superficial appearance of a flow to decide how the energy is supplied, and whether the flow will be turbulent. With the above ideas in mind, it is instructive to reconsider some aspects of flows near solid boundaries which bear on the generation of turbulence.

For all large scale natural flows of this kind (for example the wind flowing over the ground), the maintenance of turbulence can be taken for granted if the Richardson number criterion permits it. Such flows are extreme examples of those whose stability was discussed in §4.2, and provided the Reynolds number is large, this

latter parameter no longer enters the problem explicitly. (This assumption is the starting point of §5.1.) It is always necessary, however, to consider whether or not there is a buoyancy flux through the boundary, and the precise way in which the stress is transmitted to the fluid.

When the boundary flux is small, and the surface is 'aerodynamically rough', the stress is applied through the overlapping of the turbulent wakes of individual roughness elements, in a region of essentially homogeneous flow. The same is often true of much larger irregularities on a boundary: as pointed out by Davis (see §3.1.4), separation can occur behind rugged mountains and tall buildings, resulting in a direct, local injection of turbulent energy into the flow downstream.

The theories of lee waves described in §§2.3 and 3.1 assume on the contrary that the flow remains attached to the boundary, and that a stable density gradient extends right to the ground. The latter condition, which implies that heat is being extracted at the ground, provides some physical justification for the assumption that separation does not occur when the circumstances are right. Thus the sudden onset of lee waves over some ranges of hills in the evening can be attributed to a change between separated and unseparated flow. During the day convection off a heated mountain will encourage separation, whereas cooling after sunset can produce a katabatic wind (§6.2) in the lee which attaches the flow, and allows the wave motions to be set up. Much of the momentum put into the flow at the boundary can in this case be carried into the interior, only later producing turbulence in the various ways described in following sections.

Other turbulence-producing phenomena which are more directly associated with the flow over obstacles are described in chapter 3. When a stratified airflow blows over a mountain with supercritical velocity (so no lee waves can be formed), an internal hydraulic jump can occur over a horizontal plane downstream. A large amount of energy is lost during this process, and it can appear in several forms. In strong jumps, most of it is in the form of turbulent kinetic energy, some of which is used for mixing (§6.2.3). In weaker jumps, some energy is radiated away in the form of waves (on an interface or into the body of the fluid) which are not now strictly lee waves. A

spectacular example of this effect is the cloud formed behind the Sierra Nevada range (see fig. 3.11 pl. VI). A related phenomenon is the head wave behind a nose or small front (§3.2.5). Here, too, a consideration of the momentum balance shows that energy must be dissipated, and it is probably better to regard the generation of turbulence in this region as a property of the whole flow rather than the result of a local shear instability.

4.3.3. *Shear instabilities produced by interfacial waves*

In this and the following sections it will be assumed that internal waves of various forms have by some unspecified means been produced in the interior of a stratified fluid. We examine the possible mechanisms for the breakdown of such waves, first at an interface and later with continuous stratification. Internal waves certainly cannot 'break' in the same way as surface waves. For the surface wave mechanism to be relevant, the downward accelerations must be comparable with the acceleration due to gravity g (not g'), and before such a condition can be approached for internal waves, they will already have become unstable for other reasons.

In §2.1.1 it was shown that the passage of an internal wave along a sharp boundary between stratified layers produces a vortex sheet at the interface. When the wave period is long compared to the time needed for any disturbances to grow, this flow can be regarded locally as quasi-steady, and an instability of the K–H type is to be expected, as described in §4.1.2. When the interfacial region is more spread out, the vorticity produced by the internal wave will also be distributed, and the criterion for instability must depend on the gradient Richardson number (§4.1.3). Phillips (1966*a*, pp. 168, 187) showed how one can relate Ri to the properties of the wave which gives rise to the shear; we will summarize his argument and then discuss some of the limitations on its use.

We are interested in the shear through a region where the buoyancy frequency N^2 is varying, and so (2.2.6) is taken as the starting point. The amplitude of the vertical and horizontal velocities associated with a wave are related through the continuity equation

$$\frac{\partial \hat{w}}{\partial z} = -ik\hat{u}(z). \tag{4.3.1}$$

On substitution in (2.2.6) this gives

$$\left.\begin{aligned}\frac{\partial \hat{u}}{\partial z} &= -\mathrm{i}\left\{\frac{N^2(z)}{\omega^2} - 1\right\} k\hat{w} \\ &= -\left\{\frac{N^2(z)}{\omega^2} - 1\right\} \omega k a,\end{aligned}\right\} \tag{4.3.2}$$

where a is the amplitude of the vertical displacement. The maximum value of the shear occurs where $N(z)$ is a maximum (say $N = N_{\mathrm{m}}$) and (for travelling waves) near the crests and troughs. There is a local minimum of the Richardson number here, given by

$$Ri = \frac{{N_{\mathrm{m}}}^2}{(\partial \hat{u}/\partial z)^2} = \left(\frac{N_{\mathrm{m}}}{\omega} - \frac{\omega}{N_{\mathrm{m}}}\right)^{-2} (ka)^{-2}. \tag{4.3.3}$$

When $\omega \ll N_{\mathrm{m}}$ and the wavelength is large compared with the interface thickness, the shear can be regarded as steady, suggesting the use of the stability criterion $Ri_{\mathrm{crit}} = \frac{1}{4}$. (This value was shown in §4.1.3 to be appropriate for interfaces produced by diffusive spreading far from boundaries.) Applying this condition to (4.3.3), the shear flow associated with a wave of wavenumber k and amplitude a should be unstable if

$$ka > 2\omega/N_{\mathrm{m}} \tag{4.3.4}$$

which can be quite a small slope. Notice that for a given density difference *thin* interfaces and hence *large* N_{m} make the interface more unstable to this kind of disturbance, because the shear is also proportional to the density gradient but enters as the square in the denominator of (4.3.3) (cf. the tilted tube experiments of §4.1.4).

Though the above model describes the most important qualitative feature of interfacial stability, the relation (4.3.4) is probably not a satisfactory single criterion for several reasons. The time factor is important too: Ri must be lower than the limiting value and stay subcritical long enough for significant growth to take place before the wave passes by. It is not clear either that it is sufficient to consider only the region near the local (central) minimum of Ri. The horizontal velocity associated with a first mode internal wave will have other inflexion points in the deeper layers on each side where the density gradient (and hence Ri) is small. It may in fact be essential to consider the profiles as a whole before one can say when

and where a breakdown first occurs. More work is also needed before we can claim to understand the other limit of short steep waves with frequency comparable with N_m.

Beautiful observations of this kind of instability have been made in the ocean by Woods (1968*b*). Using skin diving techniques, he has shown that the seasonal thermocline near Malta is characteristically made up of a series of 'layers' in which the temperature gradient is weak, separated by thin interfaces or 'sheets' where the gradients are much larger (see chapter 10 for further discussion of this structure). When an interface is marked with dye and a train of long waves passes along it, shorter waves of the K–H type can be observed to grow at the crests or troughs. The photographs reproduced in fig. 4.20 pl. IX and fig. 4.21 pl. X show that eventually there is a breakdown to give a patch of turbulence which thickens the interface locally. The observations are in reasonable agreement with the theoretical predictions based on the interfacial structure both for the wavelength (cf. (4.1.9)) and the growthrate. There is sometimes a preferential growth at the crest or trough alone, because of the asymmetry introduced by a steady mean shear.

The energy dissipated by turbulence generated in this way comes from the internal waves, and so this provides a mechanism for limiting their amplitude (as breaking does for surface waves). Phillips (1966*a*, p. 188) has gone further, and based a calculation of the form of a 'saturated' interfacial wave spectrum on this hypothesis. This will not be pursued here, but we note that, even without taking into account any change in amplitude of the basic waves, the instability must be self-limiting, because as the interface spreads out, the energy supplied by the shear is no longer sufficient to mix fluid against the stabilizing effect of the stratification (cf. § 10.2.3).

Shear flow instabilities have also been observed (in the laboratory) associated with standing waves, for which the maximum shear is now at the positions of maximum slope (§ 2.1.3). Carstens (1964) produced the lowest order internal seiche in a long closed tank containing two immiscible fluids, by oscillating the tank horizontally. He observed a K–H type of instability close to the conditions predicted by his theory (which included surface tension), and also showed that the theoretically possible class A disturbance (see § 4.1.1) did not have time to grow to an observable amplitude. Thorpe

(1968*a*) produced much shorter, steeper, internal waves using oscillating plungers at the ends of an experimental tank, and observed a breakdown of the interface between two layers of miscible fluids. One of his photographs is shown in fig. 4.22 pl. XII; the overturning at the node rather than the crest is very clear.

4.3.4. *The interaction between wave modes*

Another kind of interfacial instability has already been mentioned in §2.4.2, which arises from a resonant action between interfacial modes. At first sight its effect on mixing at the interface may appear similar to that produced by the shear mechanism (see fig. 2.18), but the conditions for breakdown are quite different. Note again the result first obtained by Keulegan and Carpenter (1961), who observed such disturbances only when the interface thickness became *larger* than some critical value (for fixed k and a), the exact opposite of the behaviour predicted by (4.3.4). Interaction between a resonant triplet of waves on an interfacial layer leads to instability in the following way. Energy is fed from the basic wave to the other modes, which can grow exponentially from a small initial amplitude and become manifest as a growing disturbance to the original wave. The most prominent feature of the disturbance shown in fig. 2.18 pl. III is clearly of the second mode (and see also fig. 3.3). The ultimate breakdown to turbulence occurs in the form of an overturning motion, which results from the distortion of the second mode by the shear associated with the original mode.

The criterion for growth of a disturbance depends on viscosity, since the rate of transfer of energy between modes must be at least great enough to overcome viscous dissipation. For comparison with (4.3.4), we record the form of the critical slope for the first mode with wavenumber k_1 on an interface with density profile $\rho \propto \tanh z/L$; according to Davis and Acrivos (1967*b*) this is

$$(ak)_{\text{crit}} = 2\nu(g\delta)^{-\frac{1}{2}} L^{-\frac{3}{2}} F(m). \tag{4.3.5}$$

Here $\delta = \frac{1}{2}\ln(\rho_{\max}/\rho_{\min})\,(= \frac{1}{2}\rho'/\rho_{\max}$ for small density differences), L is a measure of the interface thickness and F is an increasing function of the smaller wavenumber m of the two which interact with k_1 ($F(m) \approx 1.7$ when $m = 2$). This form is clearly consistent

with the observations that, of all the possible waves formed by triplet interactions, the low wavenumber disturbances are the ones observed, and appear at smaller amplitudes when L is larger.

Two calculations which involve both the resonance mechanism and a mean shear flow should also be mentioned here. Kelly (1968) has considered spatially periodic disturbances superimposed on a particular stratified antisymmetric shear layer, and showed that resonance can lead to a growth in time of two-dimensional waves having twice the wavelength and half the frequency of the periodic component. Their growthrate is faster than that of the most unstable disturbance on the mean flow, provided the amplitude of the imposed wave is large enough; such waves nevertheless draw their energy from the basic flow.

Craik (1968) has predicted a strong 'resonant' instability at a sharp density interface which can be initiated by an interfacial wave. The mean flow considered is unidirectional, with constant velocity gradients which must be sufficiently large but unequal in the two layers. For a basic wave travelling in the direction of the mean flow, the two growing waves which complete the resonant triad can have the same component wavenumber in that direction but propagate obliquely (between 60 and 90° to it). At resonance, all three waves have the same critical layer (see §4.1.1) and the bulk of the energy transfer takes place near that level. The growing waves draw their energy from the mean shear, leaving the original wave disturbance essentially unchanged, and small viscosity plays a dominant destabilizing role in the non-linear transfer process (though the unstable waves are of Class B, according to Benjamin's classification).

4.3.5. *Internal instabilities with continuous stratification*

For completeness we should also mention here the various mechanisms which can lead to the generation of turbulent patches in the interior of a stratified fluid, away from solid boundaries or sharp interfaces. These too are associated with waves propagating through the fluid, and several of them will be described more fully in §10.3.

At sufficiently large amplitudes, the streamlines associated with lee waves can become vertical (§3.1.4), and circulating regions with closed streamlines ('rotors') appear in the flow. The density dis-

tribution is overturned and so becomes unstable, and a patch of turbulence is produced by the conversion of potential energy into kinetic. This behaviour is shown clearly in Long's experiments (fig. 3.4 pl. v), and spectacular examples of this 'kinematic' type of instability are observed in the atmosphere when condensation makes the rotors visible (see fig. 4.23 pl. xi). There is in lee waves the additional possibility of a 'centrifugal' instability occurring in parts of the flow where the curvature is large, before the fluid actually overturns (Scorer & Wilson 1963).

Local, transient overturning can also be produced both by the internal resonance mechanism described in §2.4.3, and by the random superposition of waves arising from many sources, which cannot so easily be associated with particular topographical features. Energy can be concentrated through the 'critical layer' mechanism described in §2.2.3; and we should also mention now several other ways in which the energy of progressive internal gravity waves can be concentrated in a smaller mass of fluid, so increasing the amplitude and the likelihood that they will 'break'. There is the internal equivalent of surface waves approaching a beach, and transferring their energy into a layer of decreasing depth. This effect has been observed in the ocean (see Defant 1961), but it will be illustrated here using the laboratory results of Thorpe (1966*a*) who studied both the two-layer and continuously stratified cases. Interfacial waves at first steepen at the front as the lower layer becomes shallow, but unlike breakers on a free surface, the 'crests' break backwards (as shown in fig. 4.24 pl. xii); the flow up the slope behaves like the 'nose' at the front of a gravity current (§3.2.5).

The phenomena observed in the continuous case are more complicated (see fig. 4.25 pl. xii, and also compare with the results of Wunsch (1969) referred to in §2.2.2). Near the horizontal boundary, which is the free surface in this case, there is a reduction in wavelength as well as a steepening, accompanied by regions of overturning. The flow near the bottom again runs up the slope, but without forming a raised head, and the breaking process now looks more like surface breakers. After a short time, turbulent mixing near the slope begins to change the density distribution. Mixed fluid flows back into the interior in the form of layers, which are especially prominent and regular when the boundary slope β is critical

(i.e. when $\beta = \frac{1}{2}\pi - \theta$ in the notation of §2.2.2, so that the particle motions are parallel to the slope – see also Hart (1971*c*)). Mixing near a boundary, caused by this and other mechanisms, introduces another possibility: an increase in amplitude leading to breakdown will occur when internal waves propagate horizontally into a region of decreasing density gradient which can no longer sustain them. Thus waves on the thermocline can be expected to grow as they approach a well-mixed region near a shoreline.

Another geometry which can lead to the growth of wave amplitude is a channel of constant depth which converges horizontally, so increasing the energy per unit span for a wave travelling towards the narrower end. Provided the scale is large, so that the viscous damping can be kept small, and the convergence is slow enough to avoid reflection, this seems a promising, but largely unexploited, experimental technique for studying large amplitude waves far from the direct influence of a wavemaker. In just the same way, a tank with decreasing width in the vertical could be a useful device for studying the stability of the vertically propagating waves described by the ray theory of §2.2.2. (It is not known, for example, how large the amplitude can be before some kind of instability occurs, probably in the shear layers bounding the strong in-phase motions.) This latter system is analogous to an atmosphere whose density decreases strongly with height (§3.1.4); the conservation of wave energy per unit mass will lead to an increase of amplitude in both cases. Lee waves of modest amplitude near the ground, and stable to all of the mechanisms discussed here, could achieve a sufficiently large amplitude to become unstable merely by propagating upwards to a level where the density is very much reduced.